Neural modelling of the semantic predictability gain under challenging listening conditions

Anna Rysop [1]*, Lea-Maria Schmitt [2]*, Jonas Obleser [2#], & Gesa Hartwigsen [1#]

[1] Lise Meitner Research Group Cognition and Plasticity, Max Planck Institute for Human Cognitive and Brain Sciences, Stephanstrasse 1a, 04103 Leipzig, Germany

[2] Department of Psychology, University of Lübeck, Ratzeburger Allee 160, 23562 Lübeck, Germany

* both authors contributed equally

shared senior authorship

Correspondence

Jonas Obleser
Department of Psychology
University of Lübeck
Ratzeburger Allee 160, D-23562 Lübeck
Email: jonas.obleser@uni-luebeck.de
Phone: +49 (0)451 3101 3620

Gesa Hartwigsen
Lise Meitner Research Group
Cognition and Plasticity, MPI CBS
Stephanstr. 1a, D-04103 Leipzig
Email: hartwigsen@cbs.mpg.de
Phone: +49 (0)341 9940 162

Abstract

When speech intelligibility is reduced, listeners exploit constraints posed by semantic context to facilitate comprehension. The left angular gyrus (AG) has been argued to drive this semantic predictability gain. Taking a network perspective, we ask how the connectivity within language-specific and domain-general networks flexibly adapts to the predictability and intelligibility of speech. Participants repeated sentences, which varied in semantic predictability of the final word and in acoustic intelligibility. At the neural level, increasing intelligibility of highly predictable sentences led to stronger activation of left-hemispheric semantic regions including subregions of the AG (PGa, PGp) and posterior middle temporal gyrus. The behavioural predictability gain of single participants mapped onto the same regions but was complemented by increased activity in frontal and medial regions. The facilitatory influence of PGp on PGa (quantified by dynamic causal modelling) increased for highly predictable sentences. In contrast, cingulo-opercular regions showed stronger activation with increasing intelligibility only for low predictability. Critically, better individual performance in highly predictable sentences correlated with a stronger inhibitory influence of pre-SMA on right insula. These results suggest that successful comprehension in noisy listening conditions relies on an interplay of semantic regions and concurrent inhibition of cognitive control regions when semantic cues are available.

Keywords: angular gyrus, cingulo-opercular network, semantic network, predictability gain, speech in noise comprehension.

Introduction

In everyday life, we are remarkably successful in following a conversation even when background noise degrades the speech signal. One important strategy facilitating comprehension in demanding listening scenarios is the prediction of upcoming speech. Whereas rich semantic context of speech informs accurate predictions and thereby increases speech comprehension in noise, poor semantic context provides little information to build up predictions. This *semantic comprehension benefit* is a well-documented behavioural phenomenon. It can be observed in healthy young and older listeners (Obleser, Wise, Dresner, & Scott, 2007; Obleser & Kotz, 2010; Vaden et al., 2013; Vaden, Kuchinsky, Ahlstrom, Dubno, & Eckert, 2015), in hearing-impaired listeners (Holmes, Folkeard, Johnsrude, & Scollie, 2018), as well as in cochlear implant users (Winn, 2016).

Neuroimaging studies have identified several brain regions that contribute to such successful comprehension under adverse listening conditions. These regions comprise more language-specific fronto-temporo-parietal areas (Obleser et al., 2007; Obleser & Kotz, 2010; Adank, 2012; Alain, Du, Bernstein, Barten, & Banai, 2018) as well as domain-general cognitive control regions (i.e. key areas of the cingulo-opercular network; Erb, Henry, Eisner, & Obleser, 2013; Vaden et al., 2013, 2015; Vaden, Teubner-Rhodes, Ahlstrom, Dubno, & Eckert, 2017). Among these areas, the left angular gyrus (AG) has been identified as a key region sensitive to strong semantic constraints in degraded speech (Golestani, Hervais-Adelman, Obleser, & Scott, 2013; Obleser & Kotz, 2010; Obleser et al., 2007). To study such effects, previous work manipulated speech intelligibility at multiple levels of spectral degradation (i.e., noise-vocoding) and investigated the interaction of intelligibility with semantic predictability. Using such paradigms, Obleser and colleagues (2007; 2010) demonstrated that high predictability at intermediate levels of noise-vocoding increases activity in several left-hemispheric regions, including AG, medial and lateral prefrontal cortex as well as posterior cingulate cortex (PCC). Also, the left AG has been reported as the sole region that showed a significant modulation by semantic context and intelligibility of the prime word in a retroactive priming paradigm (Golestani et al., 2013). Accordingly, Clos and colleagues (2014) found that degraded sentences elicit increased activity in left AG and left middle temporal gyrus (MTG) when they are preceded by a non-degraded sentence containing relevant contextual information. Finally, Hartwigsen and colleagues (2015) used transcranial magnetic stimulation to demonstrate that the ventral portion of left AG is functionally relevant for the behavioural comprehension gain.

Together, these studies provide converging evidence for a role of the left AG in the top-down use of semantic information when the incoming acoustic signal is degraded. Yet, the functional interplay of left AG with other regions in the semantic network are unclear. Moreover, no network-level descriptors of the semantic predictability gain to comprehension are known.

The AG is considered a heterogeneous higher-level convergence zone and has been identified as one of the most consistently activated regions in studies of semantic processing (for a meta-analysis see Binder, Desai, Graves, & Conant, 2009). Structurally, the AG is connected with frontal and temporal language regions as well as domain-general areas such as parahippocampal gyrus and precuneus (Seghier, 2013). Cytoarchitectonic studies suggest that the AG can be subdivided into a rostral part (PGa) and a caudal part (PGp; Caspers et al., 2006, 2008). On the functional level, PGa has been associated with automatic domain-general goal-directed allocation of attention and episodic memory. In contrast, PGp was (inconsistently) linked to more controlled and complex semantic-specific processes irrespective of control demands (Noonan, Jefferies, Visser, & Lambon Ralph, 2013; Bonnici, Richter, Yazar, & Simons, 2016; Bzdok et al., 2016; Jung, Cloutman, Binney, & Lambon Ralph, 2017). These findings indicate that the AG in particular might play a central role in language-specific but also in domain-general cognitive operations. In the present study, we aim to probe the functional network connections of AG and differentiate the role of PGa and PGp in the processing of semantic context in degraded speech.

It has been suggested that the comprehension of degraded speech requires additional resources to maintain stable performance (Peelle, 2018). These additional resources are thought to be provided by regions that typically do not show a functional specification, such as the cingulo-opercular network. This domain-general network comprises dorsal anterior cingulate cortex/paracingulate cortex, bilateral inferior frontal cortices and anterior insulae and has been implicated in adaptive control processes subserving the flexible allocation of attentional resources (Dosenbach, Fair, Cohen, Schlaggar, & Petersen, 2008; Duncan, 2010). Using a word recognition task with words presented at various levels of multi-talker babble, a previous study demonstrated that the magnitude of activation within the cingulo-opercular network predicted the word recognition success in the following trial (Vaden et al., 2013). The recruitment of the semantic network is thought to improve comprehension most effectively when semantic context is available, whereas the cingulo-opercular network might reflect the activation of additional cognitive resources when no external linguistic cues are available (Peelle, 2018). Here, we investigate how changing task demands shape the adaptive interplay of language-specific and domain-general resources in successful speech comprehension.

Note that previous studies manipulating predictability and intelligibility of speech suffered from small samples and mainly relied on few levels of noise fixed across participants. Moreover, most of these studies used sparse temporal sampling, precluding the investigation of effective connectivity. Consequently, it remains unclear how the identified regions influence each other during successful comprehension of speech in noise. We aimed to overcome some of the previous shortcomings by performing a continuous event-related fMRI experiment with

parametrically varying, individualized intelligibility levels. Thereby, we accounted for individual differences in auditory perception and assured comparable task difficulty across participants.

Based on previous studies, we expected a facilitatory behavioural effect of semantic predictability on speech comprehension at intermediate levels of intelligibility. We hypothesized to find increased activation in left AG and other semantic regions as a neural correlate of the semantic predictability gain at intermediate levels of intelligibility. This interaction should be driven by increased effective connectivity between the AG and other semantic regions. Moreover, we expected increasing activity and within-network connectivity in the cingulo-opercular network to improve comprehension in conditions with high listening demand (i.e., intermediate intelligibility and low predictability).

As a main finding of our study, highly predictable sentences drove activity in core regions of the semantic network and increased the functional influence between subregions of the left AG. The behavioural comprehension gain was correlated with higher activity in extended regions of the semantic network at intermediate intelligibility levels. Processing of less predictable sentences drew on cognitive control regions and strengthened effective connectivity between regions within the cingulo-opercular network, while higher predictability weakened connectivity within this network. The individual degree of inhibitory influence of higher predictability on the connection from pre-SMA to right insula was associated with the individual predictability gain.

Materials and Methods

Participants

Twenty-six healthy young German native speakers took part in this study (age range: 19–29 years, *M* = 25 years; 15 females). All participants were right-handed (mean lateralization index > 90; Oldfield, 1971) and reported no history of neurological or psychiatric disorders as well as no hearing difficulties or disorders. Four additional participants were excluded due to excessive head movements during fMRI (> 1.5 times the voxel size, n = 3) or reduced task-related activity across the whole brain in the global F-test (n = 1).

Participants gave written informed consent prior to participation and received reimbursement of €10 per hour of testing. The study was performed according to the guidelines of the Declaration of Helsinki and approved by the local ethics committee at the Medical Faculty of the University of Leipzig.

Stimulus materials

In the sentence repetition task, we used the German version of the speech in noise (SPIN) corpus (Kalikow, Stevens, & Elliott, 1977; for a detailed description of the German version, see Erb, Henry, Eisner, & Obleser, 2012) to manipulate semantic predictability of sentences. The SPIN corpus contains pairs of spoken sentences: one sentence of a pair provides poor semantic context for the prediction of the final keyword ("We are very pleased with the new <u>sheets</u>."; low predictability), whereas the complement sentence provides rich context for the same keyword ("She made the bed with new <u>sheets</u>."; high predictability).

In addition to the 100 original sentence pairs, we extended the corpus by another 28 pairs which were constructed and recorded during the development of the German SPIN corpus but not included in the final corpus. To validate the predictability of keywords in those new sentences, 10 additional participants performed a written sentence completion test (low predictability: < 5 participants reported the correct keyword; high predictability: > 5 participants). Eight new sentence pairs were exclusively used in the experiment, 20 new sentences with high predictability were used in the adaptive tracking procedure. On average, sentences of the extended corpus had a duration of 2700 ms (*SD* = 240 ms; keywords: *M* = 495 ms, *SD* = 87 ms).

All sentences were embedded in spectrally speech-shaped noise preceding and ensuing a sentence by 250 ms. Spectrally speech-shaped noise was created by filtering white noise with the long-term average spectrum of all experimental sentences (e.g. Nilsson, Soli, & Sullivan, 1994). Intelligibility of sentences was manipulated relative to a constant signal intensity of noise.

Experimental Procedures

Adaptive tracking of the speech reception threshold

Prior to the experiment, we determined the signal-to-noise ratio (SNR) required for each participant to correctly repeat half of the sentences energetically masked by speech-shaped noise (i.e., speech reception threshold; SRT). In an adaptive up-down staircase procedure (Kollmeier, Gilkey, & Sieben, 1988), participants listened to 20 sentences with highly predictable keywords. After the presentation of each sentence, participants repeated the whole sentence as accurately as possible and the investigator rated the response as either correct or incorrect online. A correct repetition was followed by an SNR decrease, an incorrect repetition was followed by an SNR increase. To account for inter-individual differences in speech-in-noise comprehension and effectively modulate behavioural performance, we used SRTs as a reference for the manipulation of intelligibility in the experiment.

The tracking procedure started with an initial SNR of 5 dB and a trial-to-trial step size of 6 db. A turning point (i.e., an increase in SNR is followed by a decrease and vice versa) reduced the step size by a factor of 0.85. We determined SRT's as the average SNR on the last five trials leading to a turn point. SRTs had an average of +1.7 dB SNR (*SD* = 2.3, range: -2.1 to +6.4 dB). All sentences were presented in the MR scanner while running the fMRI sequence later used in the experiment.

Sentence repetition task

In the main experiment, participants listened to sentences varying in predictability (high vs. low) and intelligibility (-9, -4, -1, +1, +4, +9 dB sentence intensity relative to the individual SRT; Figure 1A) during fMRI. We selected intelligibility levels based on an unpublished behavioural pilot study (n = 12) which was designed to sample the full range of behavioural performance. During sentence presentation, participants viewed a white fixation cross on a black screen. With the onset of the keyword, a green traffic light appeared on the screen and indicated the start of a 5000 ms recording period. During the recording period, participants orally repeated the sentence as accurately as possible.

The intertrial interval (ITI) was randomly set between 2000 and 7000 ms and served as an implicit baseline for the fMRI analysis. In total, participants listened to 216 sentences (18 per condition) split in six blocks intermitted by pauses of 20 s each. Sentences were presented in a pseudorandomized order avoiding the repetition of one intelligibility level more than three times in a row to prevent adaptation to specific intelligibility levels.

All sentences were presented at a comfortable volume. Sound was played via MR-Confon headphones (Magdeburg, Germany) and recorded via a FOMRI-III microphone (Optoacoustics, Yehuda, Israel). Stimulus presentation was controlled by Presentation

software (version 18.0, Neurobehavioral Systems, Berkeley, USA, www.neurobs.com). The experiment lasted 50 minutes.

MRI acquisition

Whole brain fMRI data were acquired in one continuous run with a 3 Tesla Siemens Prisma Scanner and 32-channel head coil, using a dual gradient-echo planar imaging multiband sequence (Feinberg et al., 2010) with the following scanning parameters: TR = 2,000 ms; TE = 12 ms, 33 ms; flip angle = 90°; voxel size = 2.5 x 2.5 x 2.5 mm with an interslice gap of 0.25 mm; FOV = 204 mm; multiband acceleration factor = 2. In sum, 1,500 volumes were acquired per participant, each consisting of 60 slices in axial direction and interleaved order. To increase coverage of ATL regions, slices were tilted by 10° off the AC-PC line. Field maps were acquired for later distortion correction (TR = 620 ms; TE = 4 ms, 6.46 ms). Additionally, high-resolution T1-weighted images were either obtained from the in-house database if available or were acquired prior to the functional scans with an MPRAGE sequence (whole brain coverage, TR = 1300 ms, TE = 2.98 ms, voxel size = 1 x 1 x 1 mm, matrix size = 256 x 240 mm, flip angle = 9°).

Data Analysis

Behavioural Data Analysis

All of participants' spoken response recordings from the main experiment were cleaned from scanner noise using Audacity (version 2.2.2, https://www.audacityteam.org/) and transcribed by three independent raters. Half of the data sets were transcribed by two raters and Cohen's kappa coefficient (Cohen, 1960) indicated very good inter-rater reliability for final keywords ($\kappa \geq .95$). Additionally, one rater manually determined onset and duration of oral responses.

As only predictability of the final keyword but not its preceding context is explicitly manipulated in the GSPIN corpus, we limited behavioural analyses to keywords. After rating keywords as incorrect (including missing, incomplete and inaccurately inflected keywords) or correct, we calculated the proportion of correctly repeated keywords for each participant and condition.

In the behavioural analysis, we quantified the effects of predictability and intelligibility on speech comprehension. For each participant, we fitted psychometric curves to the proportion of correct keywords across intelligibility levels, separately for sentences with low and high predictability. In detail, we fitted cumulative Gaussian sigmoid functions as beta-binomial observer models using the Psignifit toolbox (Fründ, Haenel, & Wichmann, 2011) in MATLAB (version R2018b, MathWorks). To estimate all five parameters describing the function (guess and lapse rate, threshold, width and overdispersion), we applied Psignifit's default priors for

experiments with binary single-trial outcome (here: correctly vs. incorrectly repeated keyword; Schütt, Harmeling, Macke, & Wichmann, 2016).

One participant was excluded from all analyses involving behavioural data because thresholds of psychometric curves exceeded the range of intelligibility levels tested in the experiment. As indicated by model R^2 for the proportion correct data, the goodness of fit was very good for all remaining psychometric curves of sentences with high (*M* = 0.97, *SD* = 0.03, range: 0.88-0.997) and low predictability (*M* = 0.96, *SD* = 0.04, range: 0.85-0.998).

As all 12 experimental conditions thus become subsumed in two psychometric curves, interaction effects can be evaluated by comparing parameter estimates between curves for sentences with low and high predictability. The threshold represents the intelligibility level at which participants correctly repeat half of the keywords. Keeping all other parameters constant, a threshold shift to the left indicates a comprehension gain at intermediate but not high and low intelligibility levels. We hypothesized that the interaction effect of intelligibility and predictability manifests in a smaller threshold for sentences with high predictability when compared to low predictability. Additionally, we expected that an increase in intelligibility leads to a stronger comprehension gain for sentences with high relative to low predictability. The sensitivity to changes in intelligibility is reflected by the slope which is inversely related to the width and here describes the steepness of a psychometric curve at a proportion correct of 0.5.

To explore whether also other parameters of the psychometric curves were modulated by the predictability of sentences, we compared guess and lapse rate (i.e., lower and upper asymptote) as well as width between sentences with high and low predictability. Parameter estimates were contrasted using a paired-sample *t*-test or a Wilcoxon signed-rank test whenever the assumption of normality was not met. Further, we evaluated how two parameters both significantly modulated by predictability relate to each other by computing non-parametric Kendall's τ on differences between estimates in sentences with low and high predictability.

We quantified the strength of evidence in favour of our hypotheses by calculating the Bayes Factor (BF; Jeffreys, 1961) for all *t*-tests and correlations carried out in the behavioural analyses using the default settings in JASP (i.e., comparing against a Cauchy prior with scale = $\sqrt{2}$ / 2; version 0.8.6.0). Whereas BF_{10} = 1 supports neither the alternative nor the null hypothesis, BF_{10} > 3 indicates increasingly substantial support for the alternative hypothesis (Kass & Raftery, 1995). For BF_{10} = 3, the data are 3 times more likely to have occurred under the alternative hypothesis than the null hypothesis. As an additional effect size measure, we report Pearson's correlation coefficient *r* (Rosenthal & Rubin, 1994).

Functional MRI Data

Functional MRI data were analysed using the Statistical Parametric Mapping software (SPM12, version 7219, Wellcome Department of Imaging Neuroscience, London, UK) and MATLAB (version R2017b). Preprocessing steps were applied in line with SPM's default settings and comprised realignment, distortion correction, segmentation, co-registration to the individual high-resolution structural T1-scan and spatial normalization to the MNI template while keeping the original voxel size. Volumes were smoothed using a 5 mm full width at half maximum (FWHM) Gaussian kernel to allow statistical inference based on Gaussian random-field theory (Friston, Worsley, Frackowiak, Mazziotta, & Evans, 1994). Realignment parameters were obtained from the first echo. Temporal signal-to-noise ratio (tSNR) maps were calculated for each echo based on the first 30 volumes of each participant. Echoes were combined using the information from the corresponding tSNR maps as weighting factors and realigned to the first scan. This approach has been proposed to increase SNR in brain regions typically suffering from signal loss (e.g., anterior temporal lobe regions; see Halai, Welbourne, Embleton, & Parkes, 2014 for a similar approach). Motion parameters were calculated from the parameters obtained by realignment. Additionally, framewise displacement (FD) as described by (Power, Barnes, Snyder, Schlaggar, & Petersen, 2012) was calculated as an index of head movement. Volumes that exceeded a FD of 0.9 (Siegel et al., 2014) were included as nuisance regressors.

At the single-participant level, we set up a general linear model (GLM). For each experimental condition, onset and duration of the sentence presentation period were modelled with a stick function and convolved with SPM's canonical hemodynamic response function (HRF). Additionally, we modelled onset and duration of the sentence repetition periods using individual speech onset times and speech durations. We further included motion parameters obtained from the realignment step and framewise displacement as regressors of no interest. Data were high-pass filtered with a cut-off at 128 s and serial correlations were taken into account using a first-order autoregressive model (AR(1)). Each experimental regressor was contrasted against the implicit baseline (ITI), thus yielding 12 contrast images of interest. Additionally, an F-contrast containing the experimental regressors was set up to capture experimental effects of interest and exclude effects of no interest (i.e. sentence repetition periods, motion-related activity).

At the group level, these contrasts were submitted to a random-effects (GLM RFX) flexible factorial design with the experimental factors predictability (high, low) and intelligibility (-9 to +9 dB) entered as interaction term, and an additional factor modelling the subjects' constant. First, we set up a t-contrast modelling a linear increase in intelligibility (-9 > -4 > -1 > +1 > +4 > +9 dB SNR) to reveal brain regions that are implicated in speech processing irrespective of predictability (i.e. main effect of intelligibility).

Further, we were interested in those brain regions showing a linear or quadratic interaction of intelligibility and predictability. The interaction contrasts were set up as separate t-contrasts for linearly (high > low, -9 > -4 > -1 > +1 > +4 > +9 dB SNR) and quadratically modelled intelligibility (high > low, -9 < -4 < -1 = +1 > +4 > +9 dB SNR). These parametric interaction contrasts were set up in both directions (high > low / low > high).

Single-participant's parameter estimates were extracted from significant peak voxels and transformed into percent signal change using the rfx toolbox (Gläscher, 2009) for illustration purposes. Figures were created using MRIcroGL (www. mricro.com, version v1.0.20180623).

All reported effects for the whole-brain group analysis are reported at a voxel-level family-wise error (FWE) correcting threshold of $p < 0.05$ to control for multiple comparisons. A cluster extent of at least 20 or 10 voxels was used for the main effect and the interaction, respectively. Local maxima are reported in MNI space. We used the SPM Anatomy Toolbox (Eickhoff et al., 2005, version 2.2c) and the Harvard-Oxford cortical structural atlas (https://fsl.fmrib.ox.ac.uk/fsl/fslwiki) to classify the anatomical correspondence of significant voxels and clusters.

Brain–Behaviour Correlation

We identified brain regions reflecting the behavioural predictability gain across intelligibility levels by correlating neural response patterns with task performance. On the behavioural level, we extracted the proportion of correctly repeated keywords in each experimental condition and participant as modelled by psychometric curves.

To quantify how strongly the proportion correct in each intelligibility level was affected by the predictability of sentences, we projected task performance to the interaction subspace: the condition-wise proportion correct of each participant was multiplied with the F-contrast of the interaction effect between intelligibility and predictability (for a detailed description see Henson, 2015). This procedure yielded the proportion of variance in performance explained by the interaction, i.e. the predictability gain (or loss) in each intelligibility level.

On the neural level, we limited our analysis to all voxels consistently implicated in task-related activity as indicated by a significant F-contrast ($p_{\text{uncorrected}} < 0.05$) calculated across single-participant parameter estimates of all experimental conditions (see section 2.4.2.2). For each voxel within the mask, we correlated single-participant behavioural predictability gain and neural parameter estimates across conditions. After applying Fisher's z-transformation to all Pearson product-moment correlation coefficients, single-participant maps were submitted to the Local Indicators of Spatial Association (LISA) group-level one-sample *t*-test (Lohmann et al., 2018). LISA is a threshold-free framework that allows to find consistent effects in small brain regions by applying a non-linear filter to statistical maps before controlling for multiple

comparisons at a false discovery rate (FDR) < 0.05. Voxel-wise FDR scores were obtained from a Bayesian two-component mixture model in which filtered statistical values are compared to a null distribution based on 5000 permutations (i.e., randomly switching signs of statistical maps in participants).

Dynamic Causal Modelling (DCM)

To investigate condition-specific interactions between brain areas, we conducted two separate bilinear one-state deterministic Dynamic Causal Modelling (DCM) analyses using the DCM 12.5 implementation in SPM 12. DCM is a forward-model-based method that models the dynamics of hidden neuronal states within a predefined set of regions and relates them to the measured BOLD signal (Friston, Harrison, & Penny, 2003). Using this Bayesian framework, modulations of effective connectivity by experimental conditions can be assessed.

Seed region selection

According to our main hypothesis, we were interested in the neural network dynamics underlying the predictability gain in speech in noise processing and the role of left angular gyrus. In the GLM analysis, we found two distinct networks implicated in the neural interaction of predictability and intelligibility: the semantic network and the cingulo-opercular network (CO). Here, we test effective connectivity in a subset of regions within each network. The semantic model was based on the GLM interaction contrast (high > low, linearly modelled intelligibility) and included left pMTG, PGa and PGp as seed regions. This model specification allowed to investigate differential contributions of subregions within AG, namely PGa and PGp. Based on the opposite GLM interaction contrast (low > high, linearly modelled intelligibility), we specified the CO model including pre-SMA/paracingulate gyrus as well as left and right anterior insula as seed regions.

For each subject, we identified the peak voxel nearest to the group maximum of each seed region within a sphere of 10 mm using the appropriate first-level contrast. Individual timeseries of each region (summarized as the first eigenvariate) were extracted from all voxels within 6 mm spheres (volumes of interest, VOIs) centered on the individual maximum and exceeding the liberal threshold of $p_{\text{uncorrected}} < 0.05$. The extracted timeseries were adjusted to the respective effects-of-interest F-contrast to exclude variance of no interest. The exact anatomical localization of individual seed regions was verified using SPM's Anatomy Toolbox. For the semantic model, we made sure that seed regions were not overlapping within each subject.

The summarized timeseries together with information about the onsets of the relevant conditions served as input for the DCM. The design matrix for the DCM analyses differed from

the design matrix used in the GLM analysis in the following way: three regressors were defined, modelling the onsets of (1) all experiment stimuli, (2) all high predictable sentences at medium-to-good intelligibility levels (-1, +1, +4, +9 dB SNR relative to SRT), and (3) all low predictable sentences at medium-to-good intelligibility levels. The first regressor served as sensory input (i.e. driving input) of the stimuli into the model. Regressors (2) and (3) were used as modulatory inputs and encoded whether the stimulus had high or low predictability. As inputs were not mean-centered, intrinsic parameter estimates can be interpreted as average connection strength in the absence of experimental manipulations (Marreiros, Kiebel, & Friston, 2008).

In the DCM analysis, we were mainly interested in the neural network dynamics underlying *context-dependent* changes in *successful* speech comprehension. Therefore, we excluded all intelligibility levels that showed no apparent second-level difference between sentences with high and low predictability in behavioural repetition accuracies as well as in parameter estimates of the interaction contrast. We also excluded intelligibility levels with average task performance below 50% in both predictability conditions. This procedure resulted in an exclusion of the two most unintelligible SNR levels (-9 and -4 dB SNR relative to SRT).

DCM model architecture

At the first-level, 84 models were specified for each subject. All models consisted of three types of parameters: (i) intrinsic connections between two nodes (unidirectional or bidirectional), (ii) changes in coupling strength between regions dependent on the experimental manipulation (modulatory effects) and (iii) direct influence of external input on a region (driving input).

For both DCM analyses, we modelled full reciprocal intrinsic connections as well as (inhibitory) self-connections. The driving input was set to either one region at a time, or all possible combinations between regions (resulting in 7 possible combinations). We allowed for predictability-dependent modulation of connections in the following way: either one connection was modulated separately or two afferent or efferent connections were modulated by predictability (12 possible combinations; see Supplementary Figure 1 for a schematic overview of the model space). Since family-level inference has been found especially useful in case of large model spaces (Penny et al., 2010), the resulting model space of 7 x 12 models was partitioned into 12 families, grouping models according to the modulatory input (i.e. within a family, the modulating connection was kept constant while the driving input was varied). We used the same model architecture for both DCM analyses.

All 84 models per participant were inverted using a Variational Bayes approach to estimate parameters that provide the best trade-off between accuracy and complexity quantified by free energy (Friston, Kilner, & Harrison, 2006; Friston, Mattout, Trujillo-Barreto, Ashburner, & Penny, 2007). At the second level, a random-effects Bayesian Model Selection procedure (RFX-BMS) was applied to identify the most probable family of models given the fMRI data

quantified by the respective exceedance probability (Stephan, Penny, Daunizeau, Moran, & Friston, 2009; Penny et al., 2010). Single-subject parameter estimates were averaged across all models within the winning family using Bayesian Model Averaging (BMA) and submitted to a one-sample t-test. The strength of the effects was quantified using the Bayes Factor. For *t*-tests and Bayes Factor we used JASP (version 0.9.1).

Finally, we investigated the between-subject relationship of behavioural comprehension and functional connectivity in the brain. For single participants, we summarized behavioural performance in sentences with low and high predictability as the area under the psychometric curve spanning all intelligibility levels included in the DCM analysis. The coupling strength of connections significantly modulated by predictability was correlated with behavioural performance in the according predictability condition.

Results

Semantic predictability benefits speech comprehension at intermediate levels of intelligibility

On average, participants repeated 66.97% of keywords correctly (*SD* = 10.49). Psychometric curves fitted to the proportion of correctly repeated keywords across intelligibility levels shifted leftwards for sentences with high predictability when compared to low predictability (Figure 1B). As reflected by a decrease of the threshold for sentences with high predictability relative to low predictability (t_{24} = -9.43, p < 0.001, r = 0.57, BF_{10} > 1,000; Figure 1C), high semantic predictability had a facilitatory effect on speech comprehension at intermediate intelligibility levels. Moreover, the lapse rate was smaller for sentences with high compared to low predictability (Z = -2.81, p = 0.005, r = 0.4), indicating a predictability gain that persisted (to a smaller degree) beyond intermediate intelligibility in the highest intelligibility level. The correlation of the differences between sentences with high and low predictability for threshold and lapse rate suggested that the lapse rate of sentences with low predictability increased in participants with a smaller predictability gain at intermediate levels of intelligibility (τ = -0.47, p < 0.001, BF_{10} = 44.84).

There was no significant difference between sentences with low and high predictability for slope (t_{24} = 1.47, p = 0.153, r = -0.1, BF_{10} = 0.55) and width (t_{24} = 1.73, p = 0.097, r = 0.1, BF_{10} = 0.77) or guess rate (Z = 0.07, p = 0.946, r = 0.01) of psychometric curves.

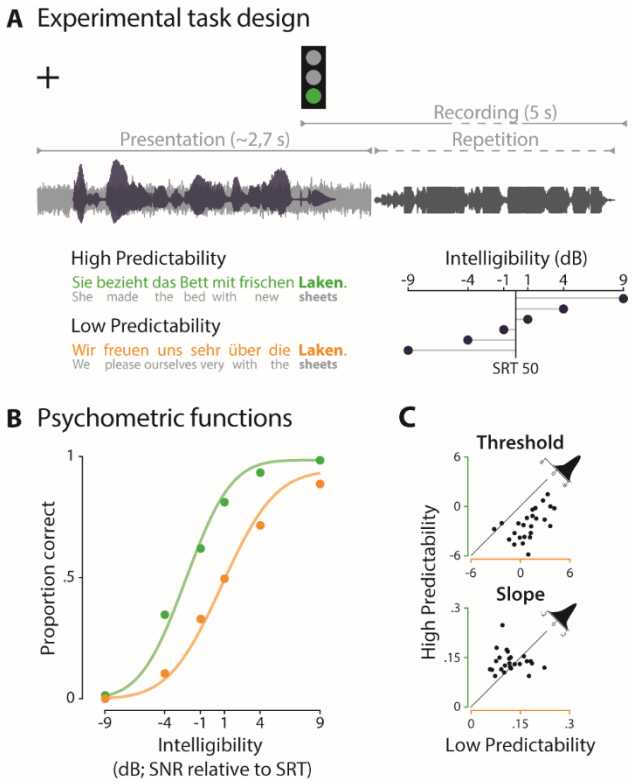

Figure 1. Design and behavioural results of the sentence repetition task. (A) In each trial, participants listened to a sentence embedded in distracting background noise while viewing a fixation cross on the screen. With the onset of the sentence's final keyword, a green traffic light prompted participants to orally repeat the whole sentence as accurately as possible within a 5 sec recording period. The preceding sentence context was either predictive (green) or non-predictive of the keyword (orange). Sentences varied orthogonally in intelligibility (ratio of speech intensity to SRT). **(B)** Psychometric functions (coloured lines) were fitted to the proportion of correctly repeated keywords (coloured dots) across intelligibility levels for sentences with low and high predictability; grand average is displayed for illustration purposes. **(C)** The threshold of sentences with low predictability shifted towards more intelligible levels when compared to sentences with high predictability ($p < 0.001$; top). There was no evidence for a slope difference between sentences with low and high predictability ($p = 0.153$; bottom). Density plots illustrate the difference between the proportion correct of sentences with high vs. low predictability.

A fronto-temporo-parietal network is tuned towards intelligible speech

First, we were interested in brain regions showing stronger activity for increasing intelligibility of speech stimuli, irrespective of sentence predictability. The parametric variation of intelligibility showed increased activation in a set of regions comprising anterior-to-posterior bilateral superior temporal gyri (STG), left precentral and postcentral gyrus (PCG) and left inferior frontal gyrus (IFG) as well as a large left-hemispheric temporo-parietal cluster and left precuneus (prec; Figure 2). These regions have previously been reported to support auditory speech comprehension and suggested to be tuned to perceptual clarity (e.g. Rauschecker & Scott, 2009).

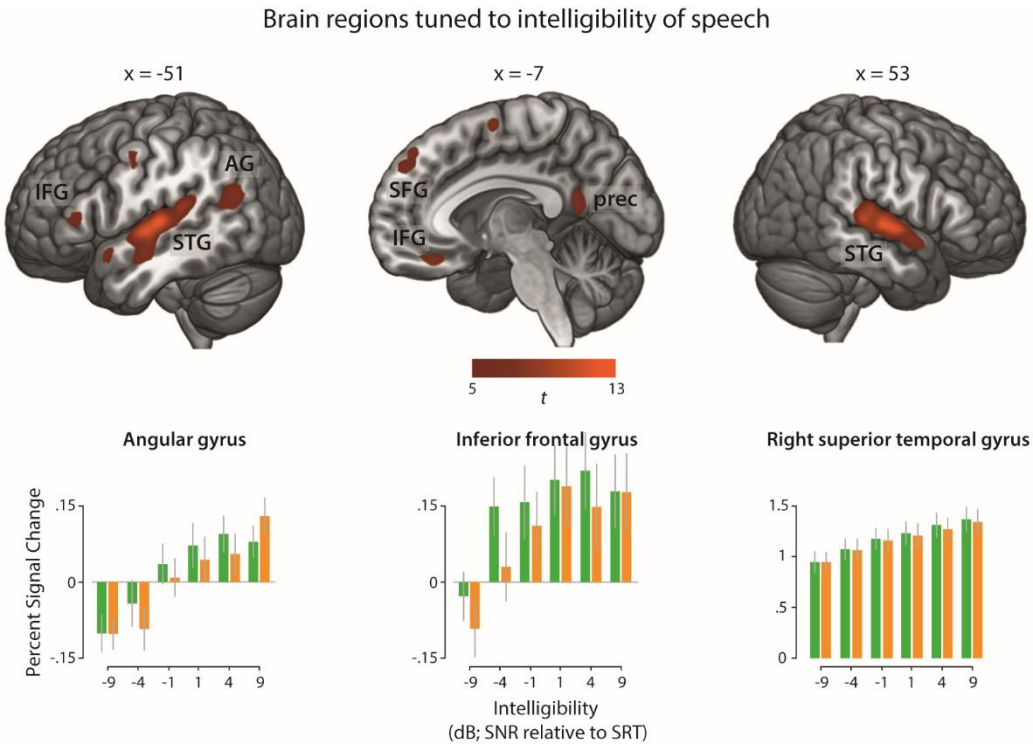

Figure 2. Main effect of increasing speech intelligibility across the whole cortex. Top: Activation map thresholded at $p < 0.05$ (FWE-corrected). STG = superior temporal gyrus, IFG = inferior frontal gyrus, AG = angular gyrus, SFG = superior frontal gyrus, prec = precuneus. Bottom: Parameter estimates (percent signal change) for each experimental condition at peak voxels of left AG (MNI: x = -47, y = -67, z = 25), left IFG (MNI: x = -54, y = 33, z = 8) and right STG (MNI: x = 53, y = -12, z = 2). Error bars represent the standard error of the mean (SEM).

Increasing intelligibility of high predictable sentences enhances recruitment of left-hemispheric temporo-parietal regions

Further, we were interested in brain regions that were differentially affected by predictability at different levels of intelligibility. Higher activation for sentences with high compared to low predictability under linearly increasing intelligibility was found in left-hemispheric regions encompassing posterior middle temporal gyrus (pMTG), middle to posterior cingulate cortex (MCC/PCC), two separate clusters in left AG (PGa and PGp), inferior temporal gyrus (ITG), precuneus (prec) and supramarginal gyrus (SMG; Figure 3, Table 1). Similar but weaker

activation patterns were found for the quadratically modulated interaction contrast. Interestingly, the two separate left-hemispheric AG clusters fell into different cytoarchitectonic subregions: the larger cluster was mainly located in the anterior dorsal portion of AG (PGa & PFm) at the boundary to SMG and the smaller cluster was mainly located in the posterior portion of AG (PGp) in close proximity to the middle occipital gyrus (MOG). The AG clusters and the pMTG cluster showed a pattern of deactivation relative to the fixation baseline with relatively less deactivation for high predictable as compared to low predictable sentences (Figure 3B). As both, the AG and pMTG are considered key regions of semantic processing, their timeseries were submitted to later connectivity analyses.

Increasing intelligibility of low predictable sentences enhances recruitment of domain-general regions

The opposite interaction contrast revealed greater activity for low compared to high predictable sentences under linearly increasing intelligibility and encompassed the pre-supplementary motor area (pre-SMA/paracingulate gyrus), left-hemispheric IFG (pars triangularis; BA 45) and the bilateral anterior insula (see Figure 3). These regions overlap with the cingulo-opercular network (Dosenbach et al., 2008), which is frequently reported in conditions associated with high task demands. To investigate context-dependent changes within this network, the pre-SMA/paracingulate gyrus and bilateral insulae were analysed in a later DCM analysis. Note that the interaction contrasts modelling intelligibility quadratically (i.e. inverted u-shape with the highest activation at intermediate levels of intelligibility) resulted in a similar pattern of brain regions and therefore are not shown here.

Table 1. Results from the context-dependent interaction.

Location	Hemisphere	MNI			*t*	Cluster Size
		x	y	z		
High > Low predictable sentences						
Middle cingulate cortex	R	3	–34	38	7.49	159
Middle cingulate cortex	L	–4	–30	42	7.17	subcluster
Middle temporal gyrus	**L**	**–60**	**–52**	**–5**	**6.85**	**150**
Middle temporal gyrus	L	–54	–62	2	6.6	subcluster
Angular gyrus (PFm/PGa)	**L**	**–42**	**–62**	**50**	**6.47**	**135**
Angular gyrus (PGa)	L	–42	–70	42	6.31	subcluster
Angular gyrus (PGp)	L	–34	–77	42	6.02	subcluster
Angular Gyrus (PGp)/ middle occipital gyrus	**L**	**–34**	**–77**	**30**	**6.34**	**51**
Angular gyrus (PGp)	L	–42	–77	28	5.63	subcluster
Supramarginal gyrus	L	–60	–30	30	5.91	26
Inferior temporal gyrus	L	–47	–52	–25	5.82	21
Angular gyrus (PGp)	R	46	–67	42	5.71	8
Precuneus	L	–10	–47	55	5.62	15
Low > High predictable sentences						
Presupplementary motor area/paracingulate gyrus	**R/L**	**0**	**16**	**50**	**7.72**	**138**
Inferior frontal gyrus (p. orbitalis, area 45)	L	–42	26	–10	6.47	106
Insular cortex	**L**	**–30**	**26**	**–2**	**6.43**	**subcluster**
Inferior frontal gyrus (p. triangularis, area 45)	L	–50	23	5	5.9	subcluster
Inferior frontal gyrus (p. triangularis, area 45)	L	–44	20	0	5.88	subcluster
Insular cortex	**R**	**30**	**26**	**–2**	**6.13**	**24**
Inferior frontal gyrus (p. triangularis, BA 45)	L	–57	20	15	5.71	16
Inferior frontal gyrus (p. triangularis, BA 45)	L	–50	20	18	5.07	subcluster

High > low predictable sentences: Regions showing greater activity for high as compared to low predictable sentences under increasing intelligibility; Low > high predictable sentences: Regions showing greater activity for low as compared to high predictable sentences under increasing intelligibility. Regions are reported at a peak-level FWE-correcting threshold at an alpha of .05. Seed regions for DCM analyses are highlighted in bold.

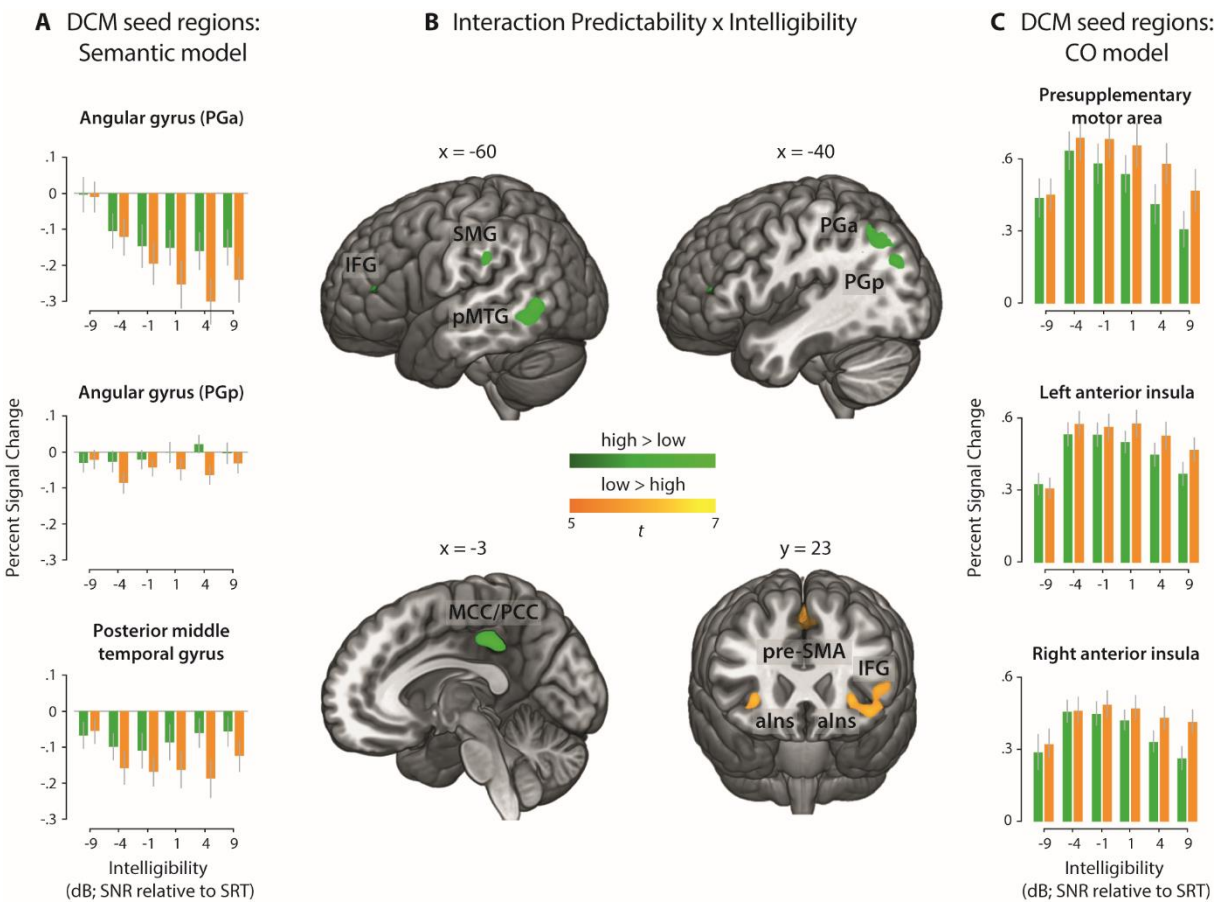

Figure 3. Group-level fMRI results illustrating brain regions that are sensitive to the interaction of intelligibility and predictability. (A) Parameter estimates illustrate the interaction effect, extracted from peak voxels of DCM seed regions for the semantic network. **(B)** Brain regions showing a significant interaction; IFG = inferior frontal gyrus, SMG = supramarginal gyrus, pMTG = posterior middle temporal gyrus, PGa = anterior angular gyrus, PGp = posterior angular gyrus, MCC/PCC = middle and posterior cingulate cortex, pre-SMA = pre-supplementary motor area, aIns = anterior insula; green = high > low predictable sentences, orange = low > high predictable sentences. The activation map is thresholded at $p_{\text{FWE-corrected}} < 0.05$. **(C)** Parameter estimates illustrate the interaction effect, extracted from peak voxels of DCM seed regions for the cingulo-opercular (CO) network.

The extended semantic system scales to the behavioural predictability gain dependent on speech intelligibility

The proportion of individual task performance explained by the interaction of predictability and intelligibility in each experimental condition correlated positively with BOLD activity in a broad semantic network (Figure 4; Binder et al., 2009). At intermediate levels of intelligibility, neural activity increased for sentences with high predictability in those participants exploiting a stronger behavioural predictability gain.

In line with the linear interaction effect (see Table 1, high > low predictability), modelling the behavioural interaction effect revealed significant clusters in parietal and lateral temporal cortex. A broad left-hemispheric and a smaller right-hemispheric cluster were observed in PGp

(Table 2). Additional clusters were found in the anterior division of left SMG as well as in bilateral posterior MTG.

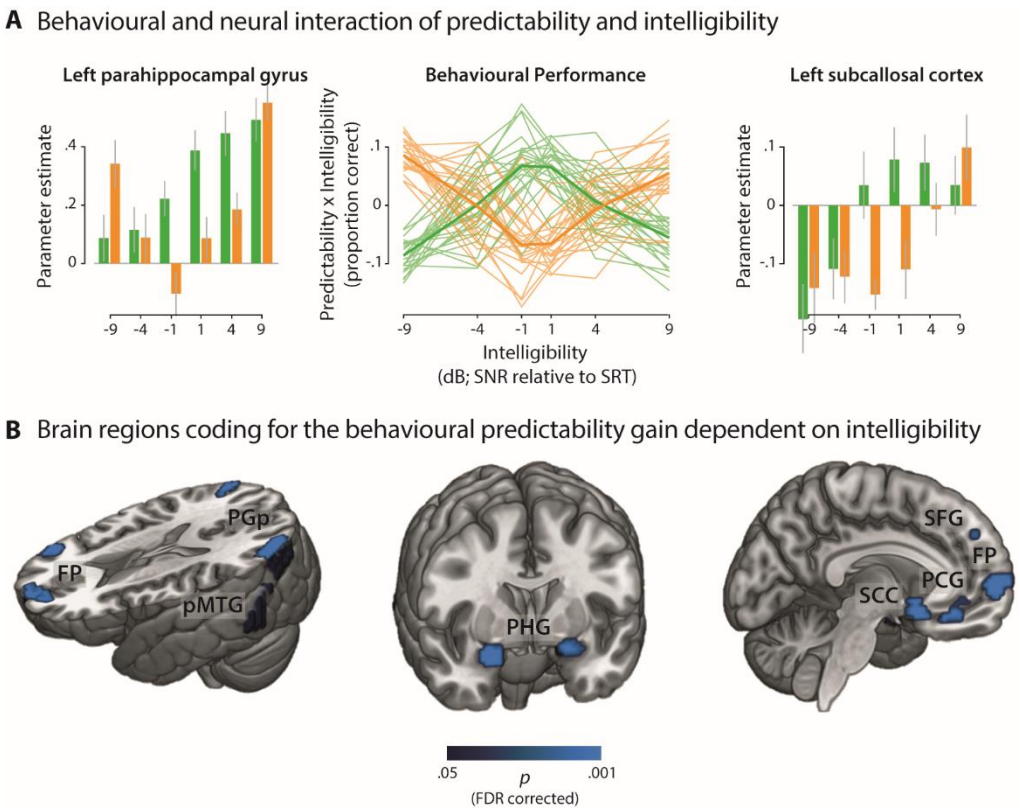

Figure 4. Projection of activity onto the behavioural predictability gain across levels of intelligibility. (A) The condition-specific proportion of behavioural performance explained by the interaction of intelligibility and predictability in each participant (middle line plot) was correlated with individual parameter estimates of single-voxel BOLD activity (left and right bar plots; exemplary grand average parameter estimates for two peak voxels). Thin lines in the line plot represent single participants; fat lines represent grand average. Error bars represent ±1 SEM. **(B)** Group statistics revealed brain areas modulated by single-participant interaction effect of intelligibility and predictability on speech comprehension. FP = frontal pole; PGp = posterior angular gyrus; pMTG = posterior middle temporal gyrus; PHG = parahippocampal gyrus; SCC = subcallosal cortex; SFG = superior frontal gyrus; PCG = paracingulate gyrus (for an exhaustive list of clusters see Table 2).

More importantly, the behavioural interaction effect mapped onto frontal and ventromedial brain regions not implicated in the linear interaction effect. The frontal pole (FP) encompassed one broad medial cluster spanning from the left to the right hemisphere as well as a right-hemispheric cluster at the border with IFG and a left-hemispheric cluster extending into the superior frontal gyrus (SFG; Table 2). Near the inferior-posterior frontal pole, we observed bilateral clusters in IFG. The limbic lobes contained a bilateral cluster in the posterior subcallosal cortex (SCC) that was complemented by an anterior cluster extending into the cingulate and paracingulate gyrus as well as the frontal medial cortex. Additional bilateral clusters comprised the anterior division of the superior parahippocampal gyrus (PHG) and the

medial-posterior insular cortex. In the medial temporal lobe, we found a left-hemispheric cluster in the posterior division of the temporal fusiform gyrus (FFG). No significant cluster in the brain showed a negative correlation with the interaction effect on task performance.

Table 2. Brain areas sensitive to the interaction effect of intelligibility and predictability on task performance.

Location	Hemisphere	MNI			*t*	Cluster Size
		x	y	z		
Brain Behaviour Correlation						
Frontal pole	L	–5	58	5	3.88	256
	R	48	38	3	4.49	121
	L	–12	56	35	3.57	20
	R	16	36	43	3.37	2
Angular gyrus (PGp)	L	–50	–70	33	3.81	205
	R	43	–70	28	3.9	109
Subcallosal cortex	L	–7	28	–15	3.8	111
	L	–7	16	–10	4.28	101
Middle temporal gyrus (temporo-occipital)	L	–60	–57	–5	3.63	104
	R	58	–45	–5	3.97	54
Parahippocampal gyrus (anterior)	R	21	1	–18	3.77	71
	L	–25	–2	–20	4.35	64
Insular cortex	L	–33	–17	5	3.67	28
	R	38	–5	–10	2.96	2
Temporal fusiform gyrus (posterior)	L	–32	–37	–13	3.86	22
	L	–42	–30	–23	3.34	4
Inferior frontal gyrus (p. orbitalis)	R	28	31	–15	3.86	16
	L	–37	36	–10	3.88	12
Supramarginal gyrus (anterior)	L	–65	–32	25	3.74	12
Planum temporale	R	56	–27	13	3.46	2

Each cluster ($p_{FDR} < 0.05$) is described by hemisphere, MNI coordinates and *t*-value of its peak voxel as well as the number of voxels it contains.

Semantic predictability increases connectivity between subregions of the angular gyrus

Next, to investigate context-dependent changes in effective connectivity between regions identified in the mass univariate GLM analysis, we performed two separate DCM analyses, one within the semantic system and one within the cingulo-opercular network.

The family of models with a context-dependent modulation of the connection from PGp to pMTG and PGa was identified as the winning family by means of Bayesian model selection (exceedance probability: 0.62; see Supplementary Figure 2A for an overview of all exceedance

probabilities). Note that the second-best family exhibited an exceedance probability of 0.09. The intrinsic connection from PGa to pMTG was negative. The remaining intrinsic connections were positive (see Supplementary Table 1), although only the outgoing connections from pMTG reached statistical significance. Within the winning family, the only significant modulatory effect was the effect of high predictable sentences on the connection from PGp to PGa (t_{25} = 2,53, p = 0.02, d = 0.5, BF_{10} = 0.51). This modulatory effect was positive (M = 0.38, SD = 0.77), indicating an excitatory influence of PGp on PGa for high predictable sentences. None of the connections was significantly modulated by low predictability, suggesting that connectivity within this network is modulated by semantic context.

Within the semantic model, we found no significant correlations between individual task performance and predictability-induced changes in connectivity strength from PGp to PGa (high predictability: r = -0.03, p = 0.893, BF_{10} = 0.25).

Semantic predictability decreases connectivity within the cingulo-opercular network

For the cingulo-opercular network model, the family of models with a modulatory effect on the connections from pre-SMA to bilateral insulae was identified as the winning family, with an exceedance probability of 0.35 (see Supplementary Figure 2B). Note that the family with modulations of the connections from pre-SMA to left insula as well as from right insula to left insula was identified as second probable family of models with an exceedance probability of 0.29.

In the winning model, both connections from pre-SMA to insula were significantly modulated by predictability (see Figure 5 and Supplementary Table 2). Low predictable sentences had on average a facilitatory effect on the connection strength, indicating increased coupling when predictability was low. Highly predictable sentences further decreased the weakly negative intrinsic connection, indicating a decrease in coupling when predictability was high.

When listening to sentences with high predictability, participants with stronger inhibitory influence from pre-SMA to right insula showed increased behavioural performance (r = -0.62, p < 0.001, BF_{10} = 43.3; Figure 5C). No significant correlations were observed between individual task performance and predictability-induced changes in connectivity strength from pre-SMA to left insula (high predictability: r = -0.11, p = 0.593, BF_{10} = 0.28; low predictability: r = -0.21, p = 0.304, BF_{10} = 0.41).

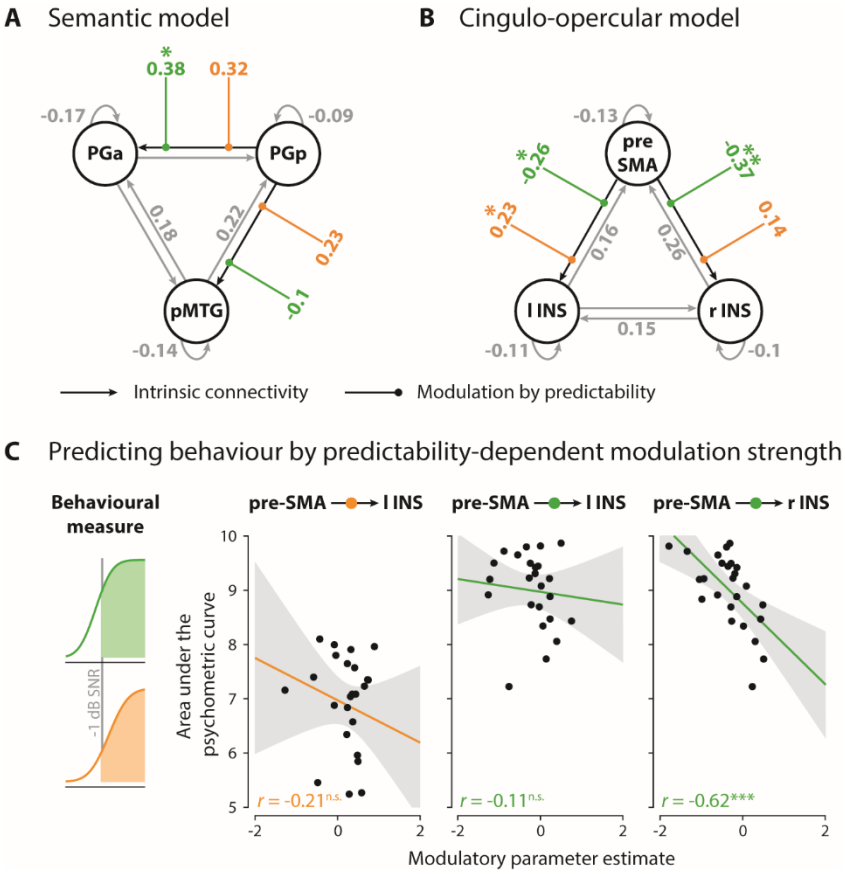

Figure 5. DCM results. Effective connectivity averaged across models within the winning family for **(A)** the semantic network and **(B)** the cingulo-opercular network. Grey arrows with parameter estimates indicate significant intrinsic connections. Black arrows indicate intrinsic connections modulated by high (green) and low (orange) predictability. **(C)** Between-subject correlation of behavioural performance (area under the psychometric curve; see illustration on the left) and modulatory connectivity strength in three cingulo-opercular connections significantly modulated by predictability; n.s. = not significant, * $p < 0.05$, ** $p < 0.01$, *** $p < 0.001$.

Discussion

In the current fMRI study, we investigated the neural underpinnings of the semantic predictability gain during speech processing in noisy listening situations at the network level. First, we show that highly predictable but acoustically degraded speech engages left-hemispheric semantic regions and modulates the individual comprehension gain in behaviour via additional frontal and medial semantic regions. Second, we found that highly predictable speech strengthens effective connectivity between two subregions of a key semantic network node in the left angular gyrus. Third, we show that highly predictable speech decreases connectivity from pre-SMA to bilateral insulae within the cingulo-opercular network. Notably, stronger decoupling of right insula predicted the individual comprehension gain. These findings suggest that semantic predictability facilitates speech comprehension in challenging listening conditions via upregulation of the semantic network and active inhibition of domain-general regions.

Our sentence repetition task had been designed to overcome the experimental shortcomings of previous studies and investigate speech comprehension in noise on the basis of rich neural and behavioural data. Hitherto, fMRI studies on the neural underpinnings of degraded speech processing had mainly used sparse temporal sampling to avoid interference of scanner noise with experimentally manipulated signal-to-noise ratio of speech stimuli (Erb et al., 2013; Golestani et al., 2013; Obleser & Kotz, 2010). As we aimed to investigate speech processing directly during (compared to after) listening and to improve sampling density for our connectivity analyses, BOLD activity in the present study was continuously recorded throughout the whole experiment. In line with studies using temporal sparse sampling (Davis & Johnsrude, 2003; Rauschecker & Scott, 2009; Abrams et al., 2013), we found activity in regions associated with auditory comprehensibility (e.g., bilateral STG as well as left IFG) to be stronger with increasing intelligibility of speech. This replication of the intelligibility effect speaks for continuous scanning as a feasible technique to investigate *online* speech processing.

Notably, in contrast to previous studies with only few and fixed experimental levels of speech degradation, we covered the full range of intelligibility from hardly to easily comprehensible speech in the individual participant. At the behavioural level, we were thus able to fit full psychometric curves (i.e., speech comprehension as a function of intelligibility, see Figure 1). We found the psychometric curve to shift towards less intelligible levels for sentences with high compared to low semantic predictability. This threshold shift is an established effect in more challenging comprehension tasks (Shannon, Fu, & Galvin, 2004) and reflects a comprehension benefit for predictable speech at intermediate intelligibility. As left AG has been found to show a strong differentiation between sentences with high and low predictability at intermediate intelligibility (Obleser et al., 2007; Obleser & Kotz, 2010) and to

exhibit functional relevance in mediating the comprehension gain (Hartwigsen et al., 2015), this region has been proposed to serve top-down activation of semantic concepts that facilitate speech comprehension (Obleser & Kotz, 2010).

However, as an unexpected finding, two separate AG clusters showed stronger activation for sentences with high compared to low predictability under linearly increasing intelligibility: a larger cluster mainly falling into PGa at the boundary to the supramarginal gyrus, and a smaller cluster at the boundary between PGp and middle occipital gyrus (MOG). Importantly, these AG subregions have been discussed to subserve different functions (Seghier, Fagan, & Price, 2010; Noonan et al., 2013; Bonnici et al., 2016). PGa is implicated in domain-general attention and converges with coordinates commonly reported as AG activation during speech in noise processing (Obleser et al., 2007; Obleser & Kotz, 2010; Clos et al., 2014; Guediche, Blumstein, Fiez, & Holt, 2014). In contrast, PGp activation has often been labelled as MOG (Guediche, Reilly, Santiago, Laurent, & Blumstein, 2016; McGettigan et al., 2012). In these studies, MOG was interpreted to provide free resources otherwise recruited by visual processing to the auditory domain during resource-demanding speech in noise comprehension. Other studies have associated PGp activation with “pure” semantic processing (Seghier et al., 2010; Bonnici et al., 2016). Our findings implicate that both AG subregions contribute to successful speech comprehension under challenging listening conditions when semantic cues are available.

To further characterize the functional contributions of anterior and posterior AG, we analysed the connectivity between these subregions and observed that coupling from posterior to anterior AG was strengthened by high but not low predictability. This finding suggests that an interplay of AG subregions enables integration of semantic information. As a semantic key region, left PGp might play an important role in integrating activated semantic information. Depending on the availability of the semantic context, PGp might recruit additional attentional resources from PGa to shift attention to semantic constraints. Aside from AG, we largely found the same regions (e.g., left pMTG, left SMG, left ITG, posterior cingulate gyrus and precuneus) that were previously implicated in processing of sentences with high predictability under increasing intelligibility (Obleser et al., 2007; Obleser & Kotz, 2010; Golestani et al., 2013). These regions overlap with the core semantic regions (Binder et al., 2009) which form a functional network during degraded speech processing (Obleser et al., 2007).

To complement the linear interaction contrast, we also modelled task performance in the brain and expected to find the left-hemispheric semantic network strengthened by this contrast fine-tuned to inter-subject variation. Indeed, the semantic core regions extended to their homologous regions in the right hemisphere. Strikingly, additional semantic regions scaled in activation with the behavioural predictability gain at intermediate intelligibility. These regions largely pertained to two subsets of the semantic network: *lateral and ventral temporal cortex* includes left temporal fusiform gyrus (FFG) and parahippocampal gyrus (PHG), whereas *left*

ventromedial prefrontal cortex includes subcallosal cortex (SCC) and frontal pole (Binder et al., 2009). The temporal cortex has been shown to communicate with the hippocampus via a connection from FFG to PHG evident in structural (Powell et al., 2004) and functional imaging (Teipel et al., 2010). It has been suggested that this pathway is used to encode semantic information (Levy, Bayley, & Squire, 2004; Martin, 2007). Critically, ventral temporal activation has been implicated in the processing of semantically unambiguous speech in a memory-demanding word recognition task (Rodd, Davis, & Johnsrude, 2005) and processing of visually presented words that were correctly repeated during later recall (Strange, Otten, Josephs, Rugg, & Dolan, 2002). In the sentence repetition task employed here, memory formation is crucial to correctly repeat the sentence after listening. The association of more accurate recall with stronger ventral temporal activation for predictable but degraded sentences suggests that memory engagement is most crucial for successful speech comprehension when semantic information is available for integration and must be protected against competing but irrelevant information (i.e., background noise). In line with this notion, prefrontal cortex regions implicated in executive control functioning (Duncan & Owen, 2000) show increased activation when efficient management of cognitive resources promises the strongest gain in performance. While we will refrain from overinterpreting these exploratory results, it is worth highlighting that the role of executive control and memory formation might have been often overlooked in previous studies on speech comprehension despite their face validity when it comes to understanding individual hearing difficulties.

As a last key finding of our study, challenging speech comprehension in the absence of semantic constraints is accompanied by an increase of activity in regions within the cingulo-opercular network. This finding is broadly in line with previous reports on activation of cingulo-opercular regions during effortful speech processing (Eckert et al., 2009; Hervais-Adelman, Carlyon, Johnsrude, & Davis, 2012; Erb & Obleser, 2013; Vaden et al., 2013; Clos et al., 2014). The cingulo-opercular network has been associated with domain-general control or executive processes such as task monitoring (e.g. Dosenbach et al., 2008; Duncan, 2010; Vaden et al., 2013, 2015), executive control (Erb et al., 2013) and attentional control (Fitzhugh, Hemesath, Schaefer, & Baxter, 2019). Specifically, in the speech in noise literature, the increased reliance on this network in difficult listening conditions has been interpreted as an adaptive control mechanism to enable speech comprehension when little or no semantic information is available. This is what we show in our study.

Within these cingulo-opercular regions, we found an inverted u-shaped response, with highest activation at intermediate levels of intelligibility and less activation for the conditions that were either hardly or easily comprehensible irrespective of predictability. This activation pattern suggests that domain-general regions contribute to effortful speech processing as long as *any* information can be extracted. Analogously, recruitment of these regions is less

important when the auditory signal is too bad or when speech is clear. Further, we observed that connectivity between these regions was differentially modulated by high and low predictability. Whereas within-network connectivity was facilitatory under low semantic predictability, highly predictable speech covaried with an inhibition in the functional interaction between these regions. These findings suggest that domain-general cognitive control regions may become actively suppressed when language-specific cues are available. An alternative interpretation outside the scope of the present methodology might be that acoustic degradation leads to an activation of this network without the assessment of alternative facilitatory cues such as semantic context, which is only taken into account in a subsequent stage.

Interestingly, the individual degree of inhibitory influence from pre-SMA to the right insula was associated with individual task performance. Those subjects who had higher comprehension scores, showed the strongest inhibitory modulation of this connection. This result converges with and extends previous task-based fMRI studies that found increased activity in the right insula when auditory input was degraded (Erb et al., 2013). While older adults with well-preserved hearing abilities and younger participants recruited the right insula under challenging listening conditions, recruitment of this region was already observed in clear speech conditions for older adults with hearing loss (Erb & Obleser, 2013).

Our results are further in line with a recent study that reported a decrease in the functional connectivity between left IFG and right insula under facilitatory neurostimulation that was associated with improved word learning (Fiori, Kunz, Kuhnke, Marangolo, & Hartwigsen, 2018). Together, the previous and present findings suggest that recruitment of the right insula is beneficial in challenging conditions (e.g. in the beginning of a learning phase or when auditory input is deteriorated) but becomes unnecessary as soon as other factors can be exploited (such as semantic context). Moreover, the present findings suggest that better behavioural performance may require an active inhibition of this region to ensure efficient processing.

Recently, the pre-SMA has been suggested to be relevant during high task demands (Hertrich, Dietrich, & Ackermann, 2016) and to play a role in the wider semantic control network (Hallam, Whitney, Hymers, Gouws, & Jefferies, 2016). In that study, the authors found increased activity in pre-SMA and pMTG after inhibitory TMS to left IFG, which was interpreted as upregulation of the relative contribution to semantic control in the presence of a TMS-induced disruption. Further, Dietrich and colleagues (2018) reported decreased performance in a sentence repetition task after inhibitory TMS over the pre-SMA, which was selectively evident for the most challenging task condition. Note that pre-SMA activation has also been reported in sentence comprehension tasks in the degraded speech literature before (e.g. Clos et al., 2014: sentence matching task) Therefore, it is unlikely that our pre-SMA finding mainly reflects the choice of the task alone. Taken together, our results replicate the previously

reported involvement of domain-general regions during effortful speech processing and extend these findings by demonstrating predictability-dependent modulation of functional connectivity within this network.

However, it is important to bear in mind that the effective connectivity results are restricted to the limited set of regions included in the network models. Furthermore, the current study investigated modulatory effects of semantic predictability on effective connectivity across medium to good intelligibility within the respective network and therefore did not operationalize the interactive effect of intelligibility and predictability per se. Future studies are needed to directly address the interactive effect and additionally investigate the dynamic interplay *between* the semantic and cingulo-opercular network.

Conclusion

Our results demonstrate that predictability in challenging listening conditions not only modulates the semantic network but critically extends to modulations in the domain-general network in a behaviourally relevant fashion. The inhibitory modulation of connectivity within the domain-general network was associated with increased behavioural speech comprehension. Further, we demonstrated that predictability modulated connectivity between two subregions of left AG. This underscores the functional heterogeneity of the AG region and emphasizes the importance of reporting findings within this region with greater regional specificity.

Funding

This work was supported by the German Research Foundation (DFG; HA 6314/4-1 and OB 352/2-1). JO is supported by an ERC Consolidator grant (ERC-CoG-2014 Grant no. 646696).

Acknowledgements

The authors would like to thank Manuela Hofmann, Sylvie Neubert and Simone Wipper for support with the data acquisition and Dagny Kühner, Isabel Gebhardt, Anna Ruhe and Ricarda Vielhauer for support with recording transcription. Conflict of interest: All authors declare no conflict of interest.

References

Abrams, D. A., Ryali, S., Chen, T., Balaban, E., Levitin, D. J., & Menon, V. (2013).

Multivariate activation and connectivity patterns discriminate speech intelligibility in

Wernicke's, Broca's, and Geschwind's areas. *Cerebral Cortex*, *23*(7), 1703–1714. https://doi.org/10.1093/cercor/bhs165

Adank, P. (2012). The neural bases of difficult speech comprehension and speech production: Two Activation Likelihood Estimation (ALE) meta-analyses. *Brain and Language*, *122*(1), 42–54. https://doi.org/10.1016/j.bandl.2012.04.014

Alain, C., Du, Y., Bernstein, L. J., Barten, T., & Banai, K. (2018). Listening under difficult conditions: An activation likelihood estimation meta-analysis. *Human brain mapping*, *39*(7), 2695–2709.

Binder, J. R., Desai, R. H., Graves, W. W., & Conant, L. L. (2009). Where is the semantic system? A critical review and meta-analysis of 120 functional neuroimaging studies. *Cerebral Cortex*, *19*(12), 2767–2796. https://doi.org/10.1093/cercor/bhp055

Bonnici, H. M., Richter, F. R., Yazar, Y., & Simons, J. S. (2016). Multimodal feature integration in the angular gyrus during episodic and semantic retrieval. *Journal of Neuroscience*, *36*(20), 5462–5471. https://doi.org/10.1523/JNEUROSCI.4310-15.2016

Bzdok, D., Hartwigsen, G., Reid, A., Laird, A. R., Fox, P. T., & Eickhoff, S. B. (2016). Left inferior parietal lobe engagement in social cognition and language. *Neuroscience and Biobehavioral Reviews*, *68*, 319–334. https://doi.org/10.1016/j.neubiorev.2016.02.024

Caspers, S., Eickhoff, S. B., Geyer, S., Scheperjans, F., Mohlberg, H., Zilles, K., & Amunts, K. (2008). The human inferior parietal lobule in stereotaxic space. *Brain Structure and Function*, *212*(6), 481–495. https://doi.org/10.1007/s00429-008-0195-z

Caspers, S., Geyer, S., Schleicher, A., Mohlberg, H., Amunts, K., & Zilles, K. (2006). The human inferior parietal cortex: Cytoarchitectonic parcellation and interindividual variability. *NeuroImage*, *33*(2), 430–448. https://doi.org/10.1016/j.neuroimage.2006.06.054

Clos, M., Langner, R., Meyer, M., Oechslin, M. S., Zilles, K., & Eickhoff, S. B. (2014). Effects of prior information on decoding degraded speech: An fMRI study. *Human Brain Mapping*, *35*(1), 61–74. https://doi.org/10.1002/hbm.22151

Cohen, J. (1960). A Coefficient of Agreement for Nominal Scales. *Educational and Psychological Measurement*, *10*(1), 37–46.

Davis, M. H., & Johnsrude, I. S. (2003). *Hierarchical Processing in Spoken Language Comprehension*. *23*(8), 3423–3431.

Dietrich, S., Hertrich, I., Müller-Dahlhaus, F., Ackermann, H., Belardinelli, P., Desideri, D., … Ziemann, U. (2018). Reduced performance during a sentence repetition task by continuous theta-burst magnetic stimulation of the pre-supplementary motor area. *Frontiers in Neuroscience*, *12*, 1–13. https://doi.org/10.3389/fnins.2018.00361

Dosenbach, N. U. F., Fair, D. A., Cohen, A. L., Schlaggar, B. L., & Petersen, S. E. (2008). *A dual-networks architecture of top-down control*. (February), 99–105. https://doi.org/10.1016/j.tics.2008.01.001

Duncan, J. (2010). The multiple-demand (MD) system of the primate brain: Mental programs for intelligent behaviour. *Trends in Cognitive Sciences*, *14*(4), 172–179. https://doi.org/10.1016/j.tics.2010.01.004

Duncan, J., & Owen, A. M. (2000). Common regions of the human frontal lobe recruited by diverse cognitive demands. *Trends in neurosciences*, *23*(10), 475–483.

Eckert, M. A., Menon, V., Walczak, A., Ahlstrom, J., Denslow, S., Horwitz, A., & Dubno, J. R. (2009). At the heart of the ventral attention system: The right anterior insula. *Human Brain Mapping*, *30*(8), 2530–2541. https://doi.org/10.1002/hbm.20688

Eickhoff, S. B., Stephan, K. E., Mohlberg, H., Grefkes, C., Fink, G. R., Amunts, K., & Zilles, K. (2005). A new SPM toolbox for combining probabilistic cytoarchitectonic maps and functional imaging data. *NeuroImage*, *25*(4), 1325–1335. https://doi.org/10.1016/j.neuroimage.2004.12.034

Erb, J., Henry, M. J., Eisner, F., & Obleser, J. (2012). Auditory skills and brain morphology predict individual differences in adaptation to degraded speech. *Neuropsychologia*, *50*(9), 2154–2164. https://doi.org/10.1016/j.neuropsychologia.2012.05.013

Erb, J., Henry, M. J., Eisner, F., & Obleser, J. (2013). The Brain Dynamics of Rapid Perceptual Adaptation to Adverse Listening Conditions. *Journal of Neuroscience*, *33*(26), 10688–10697. https://doi.org/10.1523/JNEUROSCI.4596-12.2013

Erb, J., & Obleser, J. (2013). Upregulation of cognitive control networks in older adults' speech comprehension. *Frontiers in Systems Neuroscience*, *7*, 1–13. https://doi.org/10.3389/fnsys.2013.00116

Fiori, V., Kunz, L., Kuhnke, P., Marangolo, P., & Hartwigsen, G. (2018). Transcranial direct current stimulation (tDCS) facilitates verb learning by altering effective connectivity in the healthy brain. *NeuroImage*, *181*, 550–559. https://doi.org/10.1016/j.neuroimage.2018.07.040

Fitzhugh, M. C., Hemesath, A., Schaefer, S. Y., & Baxter, L. C. (2019). Functional Connectivity of Heschl ' s Gyrus Associated With Age-Related Hearing Loss: A Resting-State fMRI Study. *Frontiers in Psychology*, *10*(November). https://doi.org/10.3389/fpsyg.2019.02485

Friston, K. J., Harrison, L., & Penny, W. (2003). Dynamic causal modelling. *NeuroImage*, *19*(4), 1273–1302. https://doi.org/10.1016/S1053-8119(03)00202-7

Friston, K. J., Kilner, J., & Harrison, L. (2006). A free energy principle for the brain. *Journal of Physiology-Paris*, *100*(1–3), 70–87. https://doi.org/10.1016/j.jphysparis.2006.10.001

Friston, K. J., Mattout, J., Trujillo-Barreto, N., Ashburner, J., & Penny, W. (2007). Variational free energy and the Laplace approximation. *NeuroImage*, *34*(1), 220–234. https://doi.org/10.1016/j.neuroimage.2006.08.035

Friston, K. J., Worsley, K. J., Frackowiak, R. S. J., Mazziotta, J. C., & Evans, A. C. (1994). Assessing the significance of focal activations using their spatial extent. *Human Brain Mapping*, *1*(3), 210–220. https://doi.org/10.1002/hbm.460010306

Fründ, I., Haenel, N. V., & Wichmann, F. A. (2011). Inference for psychometric functions in the presence of nonstationary behavior. *Journal of Vision*, *11*(6), 1–19. https://doi.org/10.1167/11.6.16

Gläscher, J. (2009). Visualization of group inference data in functional neuroimaging. *Neuroinformatics*, *7*(1), 73–82. https://doi.org/10.1007/s12021-008-9042-x

Golestani, N., Hervais-Adelman, A., Obleser, J., & Scott, S. K. (2013). Semantic versus perceptual interactions in neural processing of speech-in-noise. *NeuroImage*, *79*, 52–61. https://doi.org/10.1016/j.neuroimage.2013.04.049

Guediche, S., Blumstein, S. E., Fiez, J. A., & Holt, L. L. (2014). Speech perception under adverse conditions: Insights from behavioral, computational, and neuroscience research. *Frontiers in Systems Neuroscience*, *7*, 1–16. https://doi.org/10.3389/fnsys.2013.00126

Guediche, S., Reilly, M., Santiago, C., Laurent, P., & Blumstein, S. E. (2016). An fMRI study investigating effects of conceptually related sentences on the perception of degraded speech. *Cortex*, *79*, 57–74. https://doi.org/10.1016/j.cortex.2016.03.014

Halai, A. D., Welbourne, S. R., Embleton, K., & Parkes, L. M. (2014). A comparison of dual gradient-echo and spin-echo fMRI of the inferior temporal lobe. *Human Brain Mapping*, *35*(8), 4118–4128. https://doi.org/10.1002/hbm.22463

Hallam, G. P., Whitney, C., Hymers, M., Gouws, A. D., & Jefferies, E. (2016). Charting the effects of TMS with fMRI: Modulation of cortical recruitment within the distributed network supporting semantic control. *Neuropsychologia*, *93*, 40–52. https://doi.org/10.1016/j.neuropsychologia.2016.09.012

Hartwigsen, G., Golombek, T., & Obleser, J. (2015). Repetitive transcranial magnetic stimulation over left angular gyrus modulates the predictability gain in degraded speech comprehension. *Cortex*, *68*, 100–110. https://doi.org/10.1016/j.cortex.2014.08.027

Henson, R. (2015). Analysis of variance (ANOVA). *Brain Mapping: an encyclopedic reference. Elsevier*, 477–481.

Hertrich, I., Dietrich, S., & Ackermann, H. (2016). The role of the supplementary motor area for speech and language processing. *Neuroscience and Biobehavioral Reviews*, *68*, 602–610. https://doi.org/10.1016/j.neubiorev.2016.06.030

Hervais-Adelman, A. G., Carlyon, R. P., Johnsrude, I. S., & Davis, M. H. (2012). Brain regions recruited for the effortful comprehension of noise-vocoded words. *Language and Cognitive Processes*, *27*(7–8), 1145–1166. https://doi.org/10.1080/01690965.2012.662280

Holmes, E., Folkeard, P., Johnsrude, I. S., & Scollie, S. (2018). Semantic context improves speech intelligibility and reduces listening effort for listeners with hearing impairment. *International Journal of Audiology*, *57*, 483–492. https://doi.org/10.1097/PSY.0000000000000183

Jeffreys, H. (1961). *The Theory of Probability* (3rd Edition). Oxford: Oxford University Press.

Jung, J. Y., Cloutman, L. L., Binney, R. J., & Lambon Ralph, M. A. (2017). The structural connectivity of higher order association cortices reflects human functional brain networks. *Cortex*, *97*, 221–239. https://doi.org/10.1016/j.cortex.2016.08.011

Kalikow, D. N., Stevens, K. N., & Elliott, L. L. (1977). Development of a test of speech intelligibility in noise using sentence materials with controlled word predictability. *The Journal of the Acoustical Society of America*, *61*(5), 1337–1351. https://doi.org/10.1121/1.381436

Kass, R. E., & Raftery, A. E. (1995). Bayes Factors. *Journal of the American Statistical Association*, *90*(430), 773–795. https://doi.org/10.1080/01621459.1995.10476572

Kollmeier, B., Gilkey, R. H., & Sieben, U. K. (1988). Adaptive staircase techniques in psychoacoustics: A comparison of human data and a mathematical model. *The Journal of the Acoustical Society of America*, *83*(5), 1852–1862. https://doi.org/10.1121/1.396521

Levy, D. A., Bayley, P. J., & Squire, L. R. (2004). The anatomy of semantic knowledge: Medial vs. Lateral temporal lobe. *Proceedings of the National Academy of Sciences of the United States of America*, *101*(17), 6710–6715. https://doi.org/10.1073/pnas.0401679101

Lohmann, G., Stelzer, J., Lacosse, E., Kumar, V. J., Mueller, K., Kuehn, E., … Scheffler, K. (2018). LISA improves statistical analysis for fMRI. *Nature Communications*, *9*(1), 1–9. https://doi.org/10.1038/s41467-018-06304-z

Marreiros, A. C., Kiebel, S. J., & Friston, K. J. (2008). Dynamic causal modelling for fMRI: A two-state model. *NeuroImage*, *39*(1), 269–278. https://doi.org/10.1016/j.neuroimage.2007.08.019

Martin, A. (2007). The Representation of Object Concepts in the Brain. *Annual Review of Psychology*, *58*(1), 25–45. https://doi.org/10.1146/annurev.psych.57.102904.190143

McGettigan, C., Faulkner, A., Altarelli, I., Obleser, J., Baverstock, H., & Scott, S. K. (2012). Speech comprehension aided by multiple modalities: Behavioural and neural interactions. *Neuropsychologia*, *50*(5), 762–776. https://doi.org/10.1016/j.neuropsychologia.2012.01.010

Nilsson, M., Soli, S. D., & Sullivan, J. A. (1994). Development of the Hearing in Noise Test for the measurement of speech reception thresholds in quiet and in noise. *The Journal of the Acoustical Society of America*, *95*(2), 1085–1099.

Noonan, K. A., Jefferies, E., Visser, M., & Lambon Ralph, M. A. (2013). Going beyond inferior prefrontal involvement in semantic control: Evidence for the additional contribution of dorsal angular gyrus and posterior middle temporal cortex. *Journal of cognitive neuroscience*, *25*(11), 1824–1850.

Obleser, J., & Kotz, S. A. (2010). Expectancy constraints in degraded speech modulate the language comprehension network. *Cerebral Cortex*, *20*(3), 633–640. https://doi.org/10.1093/cercor/bhp128

Obleser, J., Wise, R. J. S., Dresner, A. M., & Scott, S. K. (2007). Functional Integration across Brain Regions Improves Speech Perception under Adverse Listening Conditions. *Journal of Neuroscience*, *27*(9), 2283–2289. https://doi.org/10.1523/JNEUROSCI.4663-06.2007

Peelle, J. E. (2018). Listening Effort: How the Cognitive Consequences of Acoustic Challenge Are Reflected in Brain and Behavior. *Ear and Hearing*, *39*(2), 204–214. https://doi.org/10.1097/AUD.0000000000000494

Penny, W., Stephan, K. E., Daunizeau, J., Rosa, M. J., Friston, K. J., Schofield, T. M., & Leff, A. P. (2010). Comparing families of dynamic causal models. *PLoS Computational Biology*, *6*(3). https://doi.org/10.1371/journal.pcbi.1000709

Powell, H. W. R., Guye, M., Parker, G. J. M., Symms, M. R., Boulby, P., Koepp, M. J., … Duncan, J. (2004). Noninvasive in vivo demonstration of the connections of the human parahippocampal gyrus. *NeuroImage*, *22*(2), 740–747. https://doi.org/10.1016/j.neuroimage.2004.01.011

Power, J. D., Barnes, K. A., Snyder, A. Z., Schlaggar, B. L., & Petersen, S. E. (2012). Spurious but systematic correlations in functional connectivity MRI networks arise from subject motion. *NeuroImage*, *59*(3), 2142–2154. https://doi.org/10.1016/j.neuroimage.2011.10.018

Rauschecker, J. P., & Scott, S. K. (2009). Maps and streams in the auditory cortex: Nonhuman primates illuminate human speech processing. *Nature neuroscience*, *12*(6), 718.

Rodd, J. M., Davis, M. H., & Johnsrude, I. S. (2005). The Neural Mechanisms of Speech Comprehension: FMRI studies of Semantic Ambiguity. *Cerebral Cortex*, *15*(8), 1261–1269. https://doi.org/10.1093/cercor/bhi009

Rosenthal, R., & Rubin, D. B. (1994). The counternull value of an effect size: A New Statistic. *Psychological Science*, *5*(6), 329–334. https://doi.org/10.1111/j.1467-9280.1994.tb00281.x

Schütt, H. H., Harmeling, S., Macke, J. H., & Wichmann, F. A. (2016). Painfree and accurate Bayesian estimation of psychometric functions for (potentially) overdispersed data. *Vision Research*, *122*, 105–123. https://doi.org/10.1016/j.visres.2016.02.002

Seghier, M. L. (2013). The Angular Gyrus. *The Neuroscientist*, *19*(1), 43–61. https://doi.org/10.1177/1073858412440596

Seghier, M. L., Fagan, E., & Price, C. J. (2010). Functional Subdivisions in the Left Angular Gyrus Where the Semantic System Meets and Diverges from the Default Network. *Journal of Neuroscience*, *30*(50), 16809 – 16817. https://doi.org/10.1523/JNEUROSCI.3377-10.2010

Shannon, R., Fu, Q.-J., & Galvin, J. (2004). The number of spectral channels required for speech recognition depends on the difficulty of the listening situation. *Acta Oto-Laryngologica*, *124*, 50–54. https://doi.org/10.1080/03655230410017562

Siegel, J. S., Power, J. D., Dubis, J. W., Vogel, A. C., Church, J. A., Schlaggar, B. L., & Petersen, S. E. (2014). Statistical improvements in functional magnetic resonance imaging analyses produced by censoring high-motion data points. *Human Brain Mapping*, *35*(5), 1981–1996. https://doi.org/10.1002/hbm.22307

Stephan, K. E., Penny, W., Daunizeau, J., Moran, R. J., & Friston, K. J. (2009). Bayesian model selection for group studies. *NeuroImage*, *46*(4), 1004–1017. https://doi.org/10.1016/j.neuroimage.2009.03.025

Strange, B. A., Otten, L. J., Josephs, O., Rugg, M. D., & Dolan, R. J. (2002). Dissociable Human Perirhinal, Hippocampal, and Parahippocampal Roles during Verbal Encoding. *The Journal of Neuroscience*, *22*(2), 523–528. https://doi.org/10.1523/JNEUROSCI.22-02-00523.2002

Teipel, S. J., Bokde, A. L. W., Meindl, T., Amaro, E., Soldner, J., Reiser, M. F., … Hampel, H. (2010). White matter microstructure underlying default mode network connectivity in the human brain. *NeuroImage*, *49*(3), 2021–2032. https://doi.org/10.1016/j.neuroimage.2009.10.067

Vaden, K. I., Kuchinsky, S. E., Ahlstrom, J., Dubno, J. R., & Eckert, M. A. (2015). Cortical Activity Predicts Which Older Adults Recognize Speech in Noise and When. *Journal of Neuroscience*, *35*(9), 3929–3937. https://doi.org/10.1523/JNEUROSCI.2908-14.2015

Vaden, K. I., Kuchinsky, S. E., Cute, S. L., Ahlstrom, J., Dubno, J. R., & Eckert, M. A. (2013). The Cingulo-Opercular Network Provides Word-Recognition Benefit. *Journal of*

Neuroscience, *33*(48), 18979–18986. https://doi.org/10.1523/JNEUROSCI.1417-13.2013

Vaden, K. I., Teubner-Rhodes, S., Ahlstrom, J., Dubno, J. R., & Eckert, M. A. (2017). Cingulo-opercular activity affects incidental memory encoding for speech in noise. *NeuroImage*, *157*(June), 381–387. https://doi.org/10.1016/j.neuroimage.2017.06.028

Winn, M. (2016). Rapid Release from Listening Effort Resulting from Semantic Context, and Effects of Spectral Degradation and Cochlear Implants. *Trends in Hearing*, *20*, 1–17. https://doi.org/10.1177/2331216516669723